PNAS
www.pnas.org

Supplementary Information for:

Brain-wide genetic mapping identifies the indusium griseum as a prenatal target of pharmacologically-unrelated psychostimulants

Janos Fuzik, Sabah Rehman, Andras G. Miklosi, Fatima Girach, Solomiia Korchynska, Gloria Arque, Roman A. Romanov, János Hanics, Ludwig Wagner, Konstantinos Meletis, Yuchio Yanagawa, Gabor G. Kovacs, Alán Alpár, Tomas G.M. Hökfelt & Tibor Harkany

Address for correspondence:

Dr. **Tomas G.M. Hökfelt** (at Karolinska Institutet; *tel*: +46 8 524 87070; *e-mail*: Tomas.Hokfelt@ki.se) or Dr. **Tibor Harkany** (at the Medical University of Vienna; *tel*: +43 1 40160 34050; *e-mail*: Tibor.Harkany@meduniwien.ac.at or Tibor.Harkany@ki.se).

This PDF file includes:

Supplementary text

Figures S1 to S11

Captions for movies S1 to S6

SI reference citations

Other supplementary materials for this manuscript include the following:

Movies S1 to S6

Supplementary Information Text

Materials and Methods

Animals and husbandry. We have generated a Scgn$^{tm1a(KOMP)Wtsi}$ (*Scgn*$^{-/-}$) mouse line which appeared anatomically normal, particularly without changes to its brain size or deformities to fine structures, including cell proliferation, migration and laminar distribution (1). We have also used GAD67$^{gfp/+}$ knock-in mice to label GABAergic interneurons in the cerebral cortex and associated structures (2). *Drd1*-GFP (MGI:3840915) and *Drd2*-GFP (MGI:3843608) brains were from GENSAT. Wild-type mice refer to the C57Bl/6N strain. Animals were group-housed under 12:12 h/h light/dark cycle with *ad libitum* access to food and water. Mice of both sexes were used for neurophysiology experiments during the period of postnatal weeks 4-9, and for behavioral experiments during weeks 8-12. Experiments on live animals conformed to the 2010/63/EU European Communities Council Directive and were approved by the Austrian Ministry of Science and Research (66.009/0145-WF/II/3b/2014, and 66.009/0277-WF/V/3b/2017). Particular effort was directed towards minimizing the number of animals used and their suffering during experiments.

Tamoxifen injection and tissue processing. *Fos*-CreER^{T2}::*ZsGreen1*$^{stop\text{-}floxed}$ 'TRAP' dams (3) were injected with tamoxifen (10mg/kg) on embryonic day (E)14.5 to induce Cre-mediated recombination. Amphetamine (10 mg/kg), nicotine (2 mg/kg), caffeine (6 mg/kg) and saline (as vehicle) were injected on E15.5 with the animals sacrificed on E17.5 (48h activation; **Fig. 1A**). The brains of both the dams and their embryos were collected and immersion fixed in 4% PFA for 24h before being immersed into 30% sucrose for cryoprotection (48h). Adult brain tissues were cut on a cryostat as 50 µm-thick serial free-floating coronal sections. Embryonic brain tissues were cut as 14 µm thickness and mounted on fluorescence free glasses.

Prenatal exposure to amphetamine. On E15, pregnant C57BL/6N females (Charles River) were intraperitoneally injected with amphetamine (10 mg/kg body weight) or saline (as vehicle) at an injection volume of 10 ml/kg. All drugs were obtained from Sigma. Animals were kept separately under standard housing conditions with a 12h/12h light/dark cycle and food and water available ad libitum. On P16 and P20, offspring from each litter was randomly selected and sacrificed for analysis. Animals were fixed by transcardial perfusion with 50 ml of phosphate buffer followed by 100-150 ml of 4% paraformaldehyde (PFA) in phosphate buffer (PB, 0.1M, pH 7.4) and processed for histochemistry as described below.

Preparation of acute brain slices. All experiments were performed in 250 µm-thick para-coronal slices (**Fig. S7**) prepared on a VT1200S vibratome (Leica) in ice-cold artificial cerebrospinal fluid containing (in mM): 90 NaCl, 2.5 KCl, 1.25 Na_2HPO_4, 0.5 $CaCl_2$, 8 $MgSO_4$, 26 $NaHCO_3$, 20 D-

glucose, 10 4-(2-hydroxyethyl)-1-piperazineethanesulfonic acid (HEPES), 3 Na-pyruvate, 5 Na-ascorbate (pH 7.4). Brain slices were then incubated at 22-24 °C for 60 min in a recording solution containing (in mM): 124 NaCl, 2.5 KCl, 1.25 Na_2HPO_4, 2 $CaCl_2$, 2 $MgSO_4$, 26 $NaHCO_3$, 10 D-glucose (pH 7.4). All constituents were from Sigma-Aldrich. Both solutions were aerated with carbogen (5% CO_2/95% O_2). Temperature in the recording chamber was set to 33 °C (TC-10, Npi). Brain slices were superfused with the recording solution at a rate of 4-6 ml/min. Neurons were visualized by differential interference contrast (DIC) microscopy on an Olympus BX51WI microscope.

Patch-clamp electrophysiology. Whole-cell recordings were carried out using borosilicate glass electrodes (Hilgenberg, Germany) of 3-4 MΩ pulled on a P-1000 instrument (Sutter). Electrodes were filled with an intracellular solution containing (in mM): 130 K-gluconate, 3 KCl, 4 ATP-Na_2, 0.35 GTP-Na_2, 8 phosphocreatine-Na_2, 10 HEPES, 0.5 ethyleneglycol-bis(2-aminoethylether)-*N*,*N*,*N*′,*N*′-tetraacetate (EGTA), (pH 7.2 set with KOH), with Cl-reversal potential ~-95 mV. Both single-cell patch-clamp recordings for cell harvesting and triple patch-clamp recordings were carried out on an EPC-10 triple amplifier (HEKA, Germany) controlled by PatchMaster 2.80. Current clamp recordings were corrected for −9.99 ± 0.38 mV liquid junction potential between the intracellular and recording solutions, as measured against a 3M KCl-electrode. Resting membrane potential (V_{rest}, expressed as mVs) was measured in current clamp mode at 0 pA current upon breaking into whole-cell configuration. Input resistance (R_m, expressed as MΩ) was calculated using linear regression established between electrotonic voltage responses (±15 mV from V_{rest}) and 500 ms current steps of increasing amplitude (10 pA increments). Membrane time constant (τ, ms) was averaged from 20 successive electrotonic voltage responses to hyperpolarizing (-40 pA) current steps and fitted with a single exponential. The sag depolarization, indicating the activation of a hyperpolarization-activated nonselective cationic current (I_h) was calculated as the ratio of the peak negative voltage and steady-state negative voltage at a voltage response to hyperpolarizing current injections resulting in a steady-state voltage of -100 mV. AP threshold (AP_{thr}, mV) was defined as the voltage point where the upstroke's slope trajectory first reached 10 mV/ms. AP rise time (ms) was the time from the AP_{thr} to the AP's peak. Maximum AP up- and AP down-strokes were determined as the maximum and minimum of the geometrical differential of the AP (mV/ms), respectively. Maximum up- and down-stroke times were the times from AP_{thr} to reach maximum AP up- and down-stroke, respectively. These parameters were measured for (*i*) the first AP elicited by a 1,000-ms rheobasic current step. Adaptation ratio was calculated as the ratio of the last 2 interspike interval relative to the first 2 interspike intervals. Firing frequency (Hz) was determined at double-threshold current injections producing spike trains. All parameters were measured by applying manual procedures custom-written in Matlab (MathWorks). We used 50 μM *Meth* (kind gift from Dr. C. Pifl, Medical University of Vienna, Austria) diluted in recording solution for acute pharmacology experiments. Histochemical

visualization of increased neuronal activity after *in vivo Meth* administration was carried out by c-Fos immunolabeling using guinea pig anti-c-Fos (1,500, Synaptic Systems; Cat No. 226 005).

Cell harvesting for RNA sequencing. At the end of each patch-clamp routine, the micropipette was voltage-clamped to a holding potential (V_{hold}) of -5 mV (4). For cell harvesting, the entire soma of each recorded neuron was aspirated into the micropipette slowly (~1 min) by applying mild negative pressure (-50 mPa). This procedure allowed us to retain a tight seal during aspiration and to minimize RNA loss by keeping RNA molecules in solution within the pipette. When we broke contact, the recording pipette was pulled out from the recording chamber and then carefully rotated over an expelling 0.2 ml tube, where its content (0.5 µl) was ejected onto a 0.5 µl drop of lysis buffer pre-placed in the 0.2 ml tight-lock tube (TubeOne). The resultant sample (1 µl) was spun down (20 s) to the bottom of the conical tube at 24 °C, stored at -80 °C and later subjected to in-tube reverse transcription (RT).

Lysis, cDNA synthesis for library preparation and RNA-sequencing. Cell aspirates were dispensed into ~0.5 µl lysis mix consisting of 0.15% Triton X-100, 1 U/µl TaKaRa RNase inhibitor, 2.5 mM dNTP, 17.5 mM DTT and oligo dT primer (2.5 uM). Samples were collected and stored at +80 °C until batch processing. Before reverse transcription, samples were thawed and lysed at 72 °C for 3 min, then cooled to 4 °C. Immediately following the lysis step, 2 µl RT mix (1× SuperScript II First-Strand Buffer; Life Technologies) supplemented with 15 mM $MgCl_2$, 2.5 µM strand-switching primer "LNA", 1.5 U/µl TaKaRa RNase inhibitor (Clontech), 1.45 M betaine and 21 U/µl Superscript II reverse transcriptase (Life Technologies)) were added and incubated at 42 °C for 90 min followed by 72 °C for 10 min. Following reverse transcription, 8 µl PCR mix (1× KAPA HiFi 2× ready mix and 80 nM ISPCR primers) were added and PCR-amplified using thermal cycling as follows: 95 °C for 3 min (5 cycles), 98 °C for 20 s, 62 °C for 4 min, 72 °C for 6 min, (9 cycles) 98 °C for 20 s, 68 °C for 30 s, 72 °C for 6 min, (7 cycles) 98 °C for 30 s, 68 °C for 30 s, 72 °C for 7 min. Subsequently, PCR samples were cleaned using AMPure-XP beads (1:1 ratio; Beckman Coulter) and quantified by Qubit (Life Technologies) on an Agilent bioanalyzer. Tagmentation and subsequent library preparation were done using the Nextera-XT kit (Illumina). Paired-end (50bp) single-cell RNA-sequencing was done on an Illumina Hiseq2500 instrument, generating ~1.5 million reads/cell. Alignment and locus mapping of the reads were done using HTseq and Bowtie 2.0.

Immunohistochemistry. For the anatomical analysis of the IG, guinea pig anti-VGLUT1, rabbit anti-VGLUT2 and rabbit anti-VGLUT3 (1:1,000; Synaptic Systems, Cat. No. 135304; Cat. No. 135403; Cat. No. 135203, respectively), guinea pig anti-NPY (1:500; Abcam, Cat. No. ab10341), rabbit anti-glial fibrillary acidic protein (GFAP, 1:1,000; DAKO, Cat. No. GA52461-2), mouse anti-myelin basic protein (MBP, 1:200; R&D Systems, Cat. No. MAB42282), mouse anti-Iba1 (1:1,000, Millipore, Cat. No. MABN92), mouse anti-ZsGreen1 (OTI2C2, 1:1,000, Thermo Fisher), rabbit

anti-Scgn (1:1,000, Atlas Antibodies, Cat. No. HPA006641), guinea pig anti-c-Fos (1,1:000, Synaptic Systems; Cat No. 226 005) and rabbit anti-*Brn*-1 (1:100, Santa Cruz, Cat. No. sc-6028) primary antibodies as well as *Solanum tuberosum* lectin (20 µg/ml; Vector Labs.) were employed according to standard protocols (2). Hoechst 33,342 (Sigma) was used as nuclear counterstain.

Tissue clearing of mouse samples, light-sheet microscopy. Freshly prepared brain slices of 500 µm were post-fixed in 4% PFA in phosphate buffer (PB, 0.1M, pH 7.8) at 4 °C overnight. Slices were repeatedly washed in PB and cleared using the CUBIC method (5) by first immersing in 'CUBIC reagent 1' (25% urea, 25% *N*,*N*,*N*′,*N*′-tetrakis(2-hydroxypropyl) ethylenediamine and 15% Triton X-100) for 2 d. Scgn immunohistochemistry started by blocking the specimens in 2% bovine serum albumin (BSA), 5% normal donkey serum (NDS) in 0.1M PB for 2h and then exposing those to rabbit anti-Scgn antibody (1:10,000) in 0.1% BSA, 1% NDS, 10% DMSO (to facilitate deep tissue penetration) on an orbital shaker at 22-24 ^{o}C for 3 days. This was followed by repeated rinses in 0.1M PB followed by exposure to a secondary antibody (Cy5-conjugated secondary antibody made in rabbit (1:200; Jackson) and at 22-24 ^{o}C for 2 days. Slices were then rewashed in PB and submerged in 'CUBIC reagent 2' (50 % sucrose, 25 % urea, 10% 2,20,20'-nitrilotriethanol and 0.1% Triton X-100) for further clearing. Cleared tissues from immunostainings or from *Fos*-CreER^{T2}-based activity mapping were imaged on a laser-scanning microscope (Zeiss LSM880) or a Lightsheet.Z1 microscope (Zeiss).

Whole brains of E17.5 embryos were cleared using a modified CUBIC protocol (6). Brain samples were initially fixed in 4% PFA for 24h, and incubated in 'CUBIC reagent 1' under continuous agitation at 37 °C for 3 days. Subsequently, the samples were washed 3x 30 min each in 0.1M PB prior to immersion in 'CUBIC reagent 2' in which they were left at 22-24 °C for 3 days before imaging. All samples were imaged in 'CUBIC reagent 2' with a measured refractory index of 1.45. Orhtogonal images were acquired on a Lightsheet Z.1 (Zeiss) microscope using a 5× detection objective, 5× illumination optics and laser excitation at 488 nm. Each plane was illuminated from a single side, and images of the whole brain were obtained through 3 × 4 tile scanning. All images were captured at 0.7× zoom, with *z*-stack intervals set at 3.5 µm with an exposure time of 600 ms. 3D-rendered images were visualized with Arivis Vision4D for Zeiss (v. 2.12). Brightness and contrast of the 3D-rendered images were manually adjusted to aid visual clarity. The distribution of ZsGreen1^{+} cells was charted on coronal sections of both E17.5 (Prenatal mouse brain atlas (Schambra, Uta)) and adult brain templates (from The mouse brain atlas (Paxinos and Franklin) using overview brain Refs. Quantitative analysis was performed in Arivis.

Tract tracing. Twelve week-old rats were anesthetized (*i.m.*) with a mixture of ketamine (50 mg/kg) and xylazine (4 mg/kg) and placed in a Kopf stereotaxic instrument. The skull was exposed by a skin incision, and burr holes at corresponding coordinates were drilled to access the brain.

Tracers were injected stereotaxically using a 1.0 µl Hamilton syringe mounted on a microinjector (Kopf). Retrograde or anterograde tracers (40 nl each) were deposited by slow pressure injection during 5 min. The needle was retracted only after a 15 min resting interval to minimize leakage. Coordinates were verified in pilot experiments by methylene blue injections (Paxinos rat brain atlas). Alexa Fluor 594-conjugated choleratoxin B subunit (*retrograde* tracer, Molecular Probes; 1% dissolved in 0.05M phosphate-buffered saline) was injected into the olfactory bulb (AP: +7 mm, L: 1 mm, DV: -1.5 mm). Alexa Fluor-594 conjugated dextran (10 kDa, D594, Molecular Probes; 10% dissolved in distilled water) was infused into the fasciola cinerea (AP: -5.5 mm, L: -0.5 mm, DV: -2.5 mm). Four and 7 days after retrograde and anterograde tracing, respectively, rats were re-anesthetized with ketamine and xylazine as above and transcardially perfused first with 50 ml physiological saline solution followed by 250-300 ml of 4% PFA in 0.1M PB (pH 7.4).

The brains were post-fixed in 4% PFA in PB at 4 °C overnight, and transferred to 30% sucrose (diluted in PB, 4 °C, for 2 days) for cryoprotection. Brains were sectioned at 40 µm thickness on a Leica freezing microtome in the saggital plane. Free-floating sections were rinsed in PB (pH 7.4), blocked in 5% NDS (Jackson), and 0.3% Triton X-100 (Sigma) in PB for 2 h at 22-24 °C, then exposed (72 h at 4 °C) to a rabbit anti-Scgn antibody (1:10,000) in PB to which 0.1% NDS and 0.3% Triton X-100 had been added. After rinsing in PB, immunoreactivity was revealed by rabbit-specific Cy2 or Cy5-tagged secondary antibodies raised in donkey (1:500 (Jackson), 24 h at 4 °C). Glass-mounted sections were coverslipped with Surgipath Micromount (Leica).

Human adult samples. We have applied direct perfusion via the internal carotid and vertebral arteries, which facilitated the preservation of tissue integrity relative to alternative fixation methods. Human brains (*n* = 2, gender and age: female/83 years and male/79 years, with a clinical history of no neurodegenerative disease, ethical approval: TUKEB 84/2014, Hungary) were first perfused with physiological saline followed by a fixative containing 2% PFA and 0.1% glutaraldehyde in 0.1 M Tris-buffered saline (TBS, pH 7.4) 7h or 11h after death. The removal and subsequent preparation of human tissues were in accordance with relevant ethical guidelines of Semmelweis University (1998, Budapest, Hungary), including informed concent. Slices containing the IG were prepared from human tissue post-fixed in 2% PFA in TBS for 72, followed by immersion in cryoprotective 30% sucrose in 0.1M PB (pH 7.4) overnight. Coronal sections (50 µm) were cut on a cryostat microtome and processed for immunohistochemistry. Free-floating sections were rinsed in PB (pH 7.4) and pre-treated with 0.3% Triton-X 100 (in PB) for 1h at 22-24°C to enhance the penetration of antibodies. Non-specific immunoreactivity was suppressed by incubating our specimens in a cocktail of 5% NDS (Jackson), 10% BSA (Sigma) and 0.3% Triton X-100 (Sigma) in PB for 1h at 22-24 °C. Sections were exposed for up to 72h (at 4 °C) to the cocktail of primary antibodies (rabbit anti-Scgn (1:5,000); mouse anti-MAP2 (1:200; Sigma) and guinea pig anti-calretinin (1:1,000; Synaptic Systems) diluted in PB to which 0.1% NDS and 0.3% Triton X-100 had been added. After extensive rinsing in PB, immunoreactivities were

revealed by chromogenic staining (as above) or by Cy2, 3 or 5-tagged secondary antibodies raised in donkey (1:200 [Jackson], 2h at 22-24 °C). Lipofuscin autofluorescence was quenched by applying Sudan Black-B (1%, dissolved in 70% ethanol (7)). Glass-mounted sections were coverslipped with Aquamount embedding medium (Dako). Sections were inspected and images acquired on a 710LSM confocal laser-scanning microscope (Zeiss) at 10x or 40x primary magnification, and pinhole settings limiting signal detection to 0.5-0.7 µm. Emission spectra for each dye were limited as follows: Cy2/505-530 nm, Cy3/560-610 nm, and Cy5/650-720 nm.

Human fetal tissue. Fetal brain tissue was obtained from spontaneous or medically-induced abortions. Only cases without genetic disorders, head injury, or neurological diseases were included. These cases showed no chromosome aberrations or *post-mortem* autolysis. Neuropathological examination excluded major central nervous system malformations, severe hypoxic/ischemic encephalopathy, intraventricular hemorrhages, severe hydrocephalus, and meningitis or ventriculitis. A 236 days old fetal brain with no disease history was then selected from the Brain Bank of the Institute of Neurology, Medical University of Vienna, Austria. All procedures were compliant with the Declaration of Helsinki and followed institutional guidelines, including maternal consent. The study was approved by the Ethical Committee of the Medical University of Vienna (No.104/2009). Three-µm-thick sections from formalin-fixed, paraffin-embedded tissue blocks containing the corpus callosum and the hippocampal formation were mounted on pre-coated glass slides (Star Frost). Shortly after deparaffinization and rehydration, the sections were pretreated in low-pH EnVision FLEX antigen retrieval solution at 98 °C for 20 min (PTLink; Dako) and subsequently incubated with rabbit anti-*Scgn* antibody (1:12,000). The DAKO EnVision detection kit, peroxidase/3,3-diaminobenzidine-tetrahydrochloride (DAB), and rabbit secondary antibody (K5007, ready-to-use; Dako) were used to visualize antibody binding. Sections were counterstained with hematoxylin, dehydrated in ascending concentrations of ethanol, cleared with xylene, and covered with Consil-Mount (Thermo Scientific). Representative images containing the area of interest were exported from scanned sections (NanoZoomer 2.0; Hamamatsu).

Behavioral experiments. Methamphetamine (kind gift of Dr. C. Pifl, Medical University of Vienna) was injected *i.p.* at a dose of 15 mg/kg in male wild-type (n = 3) and *Scgn*$^{-/-}$ mice (n = 4) (8-12 weeks of age) 3 times with 90 min intervals. All mice were tested on the same day in one cohort. The spontaneous behavioral state of each mouse was scored by 2 independent observers 30 min before the first injection (baseline) and 60 min after each methamphetamine injection using the SHIRPA protocol (8, 9). Criteria were set as follows: *body position*: 0 = inactive, 1 = active 4 paws, 2 = excessively active 2 paws, 3 = lordosis; *spontaneous activity*: 0 = none, 1 = slow movement, 2 = moderate movement, 3 = rapid movement; *respiration rate*: 0 = irregular, 1 = slow, 2 = normal, 3 = hyperventilation; *tremor*: 0 = absence, 1 = presence; *piloerection*: 0 = absence, 1 = presence; *gait*: 0 = normal, 1 = fluid but normal, 2 = limited movement, 3 = incapacity; *tail*

elevation: 0 = dragging, 1 = horizontally extended, 2 = elevated, 3 = horizontally bent; *limb grasping*: 0 = absence, 1 = present in forelimb, 2 = present in hindlimb, 3 = limb rigidity/less extended; *clonic convulsions*: number of clonic convulsions in 60 sec; *tongue stuck out*: 0 = absence, 1 = less/licking the wall on 2 paws, 2 = almost continuous. Sample videos were taken after the scoring of behavioral state at 60 min indicated as test two (T2).

Figures and statistics. Composite figures were assembled in CorelDraw X7 (Corel Corp.). Statistical analysis of data for electrophysiology and behavioral experiments was carried out in Matlab. We used the Mann-Whitney *U*-test to determine group differences whenever the Shapiro-Wilk test failed to verify normal distribution of the data; including *Meth*-induced modifications in *Scgn*$^{-/-}$ mice. Two-way ANOVA (repeated-measures design) was used to reveal progressive *Meth* effects when repeatedly dosing and testing wild-type and *Scgn*$^{-/-}$ mice. Time points (TB, T1, T2 and T3) and genotype were selected as variables. Data were processed in Matlab using its 'anova' and 'anova2' functions. Contrast analysis to identify IG-specific neuronal markers in *Patch-seq* experiments was also performed in Matlab. We used 'reads per kilo base per million mapped reads' (RPKM) data as Tasic *et al.* (10) to aid comparative assessment. We filtered the set of genes obtained from visual cortical neurons with zero or low expression (low-pass filtering) and compared these to highly-expressed genes in IG from our *Patch-seq* dataset (high-pass filtering). The open-source Allen brain atlas adult mouse *in situ* hybridization database was then used to manually filter putative marker genes.

Supplementary Figures

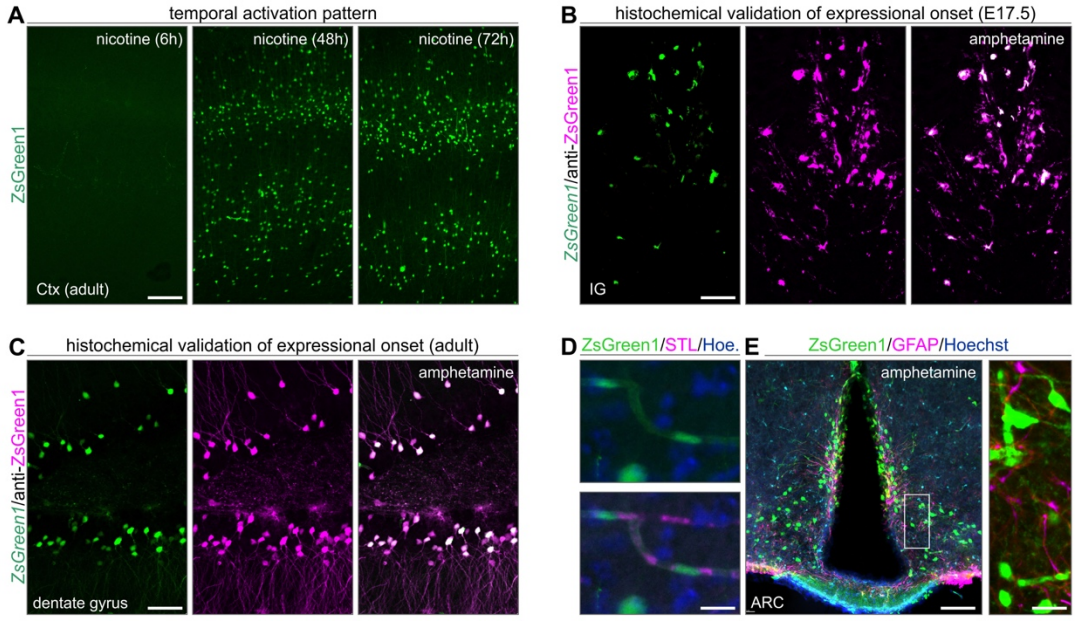

Figure S1: Methodological controls of the transgenerational 'TRAP' mouse model. (**A**) Considering that immediate early gene-CreER^{T2}-dependent models to detect transient neuronal activity rely on the coincidence of tamoxifen-induced Cre activity and the experimental manipulation, it is imperative to control if the temporal setting of the experiments allows for successful recombination. Here, nicotine is shown to induce recombination in the neocortex, with abundant ZsGreen1 expression by 48h and 72h. (**B,C**) Next, an anti-ZsGreen1 antibody with indirect fluorescence detection was used in both fetal (B) and adult (C) brains to show a virtually complete overlap with genetically-encoded ZsGreen1 fluorescence. In both cases, amphetamine was used to trigger cellular activity. (**D**) Besides neurons, ZsGreen1 signal was also seen in endothelial cells, which were labeled by *Solanum tuberosum* lectin (STL). Nuclei were counterstained with Hoechst 33,342. (**E**) Amphetamine-induced neuronal activation in the arcuate nucleus (ARC). Note that ZsGreen1 fills release terminals at the median eminence. Inset shows the relative abundance of ZsGreen1 in neurons but not astroglia (labeled for glial fibrillary acidic protein; GFAP). *Abbreviations*: Ctx, cortex; IG, indusium griseum; *Scale bars* = 200 µm (A), 50 µm (C), 30 µm (B).

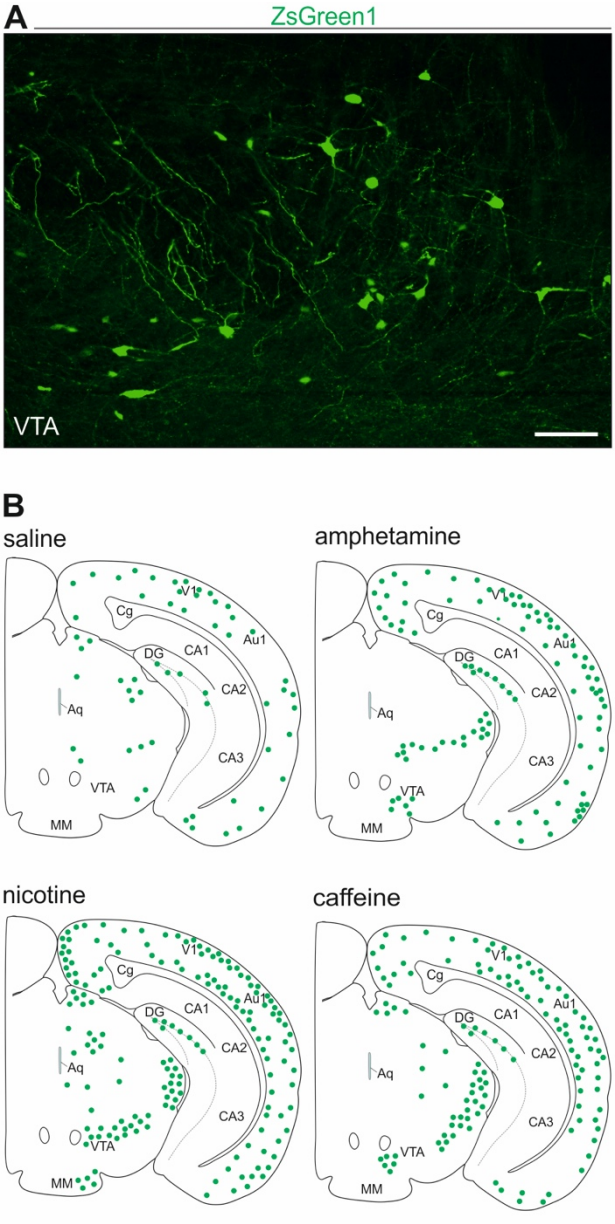

Figure S2: Neuronal activation in the ventral tegmental area upon psychostimulant exposure. (**A**) In adult *Fos*-CreER^{T2}::*ZsGreen1*$^{stop\text{-}floxed,stop\text{-}floxed}$ mice, all three psychostimulants used activated neuronal contingents in the vental tegmental area (VTA). Here, the effects of amphetamine are shown. (**B**) Distribution of *ZsGreen1*$^{+}$ neurons after amphetamine, nicotine and caffeine treatment at the coronal plain spanning the VTA. These observations served as positive control for the drug effects. *Abbreviations*: Aq, aqueduct; Au1, auditory cortex; CA1-3, Cornu Ammonis 1-3 subfields of the hippocampus; DG, dentate gyrus; MM, medial mammillary nucleus; VTA, ventral tegmental area; V1, visual cortex. *Scale bar* = 75 μm.

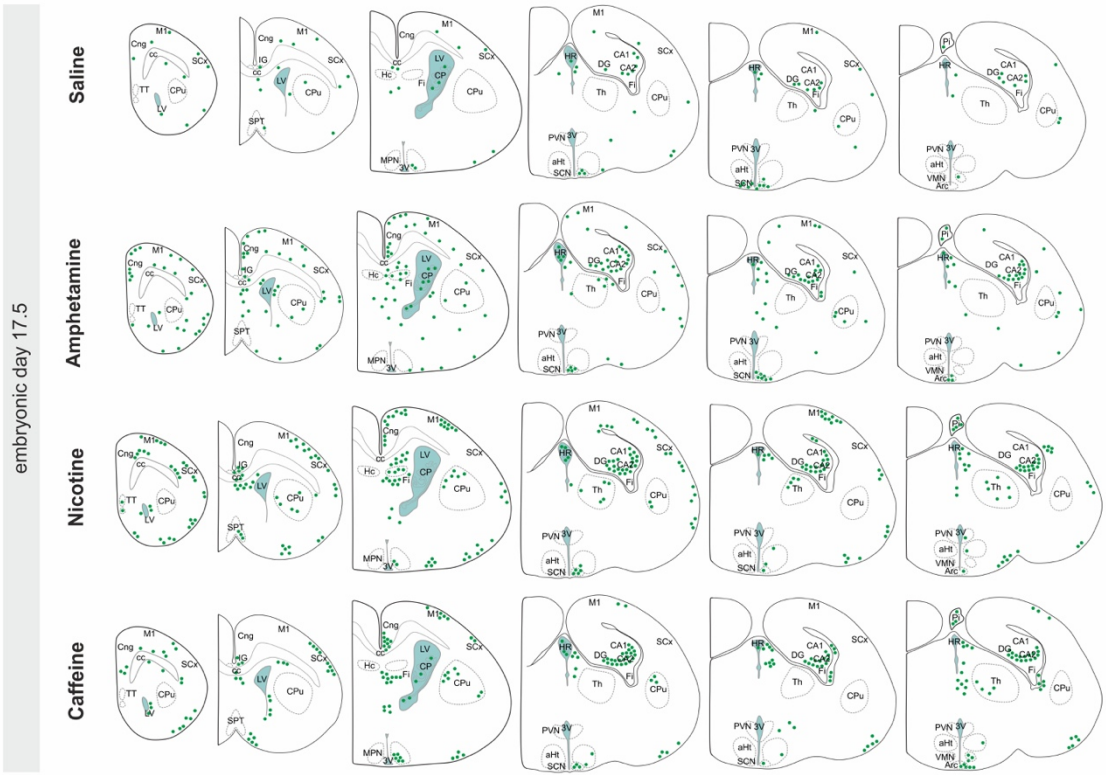

Figure S3: Cell activation maps for fetal brains. *Fos*-CreER^{T2}::*ZsGreen1*$^{stop\text{-}floxed,stop\text{-}floxed}$ mice were treated with the psychostimulants as described (**Fig. 1A**). After 72h survival, serial brain sections were analyzed to localize ZsGreen1^{+} somata (without histochemical signal amplification). Data are from $n \geq 4$ fetal brains/treatment, which were mapped by at least two independent researchers blinded to the case conditions. *Abbreviations*: aHt, anterior hypothalamus; ARC, arcuate nucleus; cc, corpus callosum; CA1,2, Cornu Ammonis 1,2 subfields of the hippocampus; Cng, cingulate cortex; CP, choroid plexus; CPu, striatum; DG, dentate gyrus; Fi, fimbria hippocampi; Hc, hippocampus; HR, habenular recess; IG, indusium griseum; LV, lateral ventricle; M1, motor cortex; MPN; median preoptic nucleus; Pi, pineal gland; PVN, parsventricular nucleus of the hypothalamus; SCN, suprachiasmatic nucleus; SCx, somatosensory cortex; SPT; septum; Th, thalamus; TT, tenia tecta; VMN, ventromedial hypothalamic nucleus; 3V, 3rd ventricle.

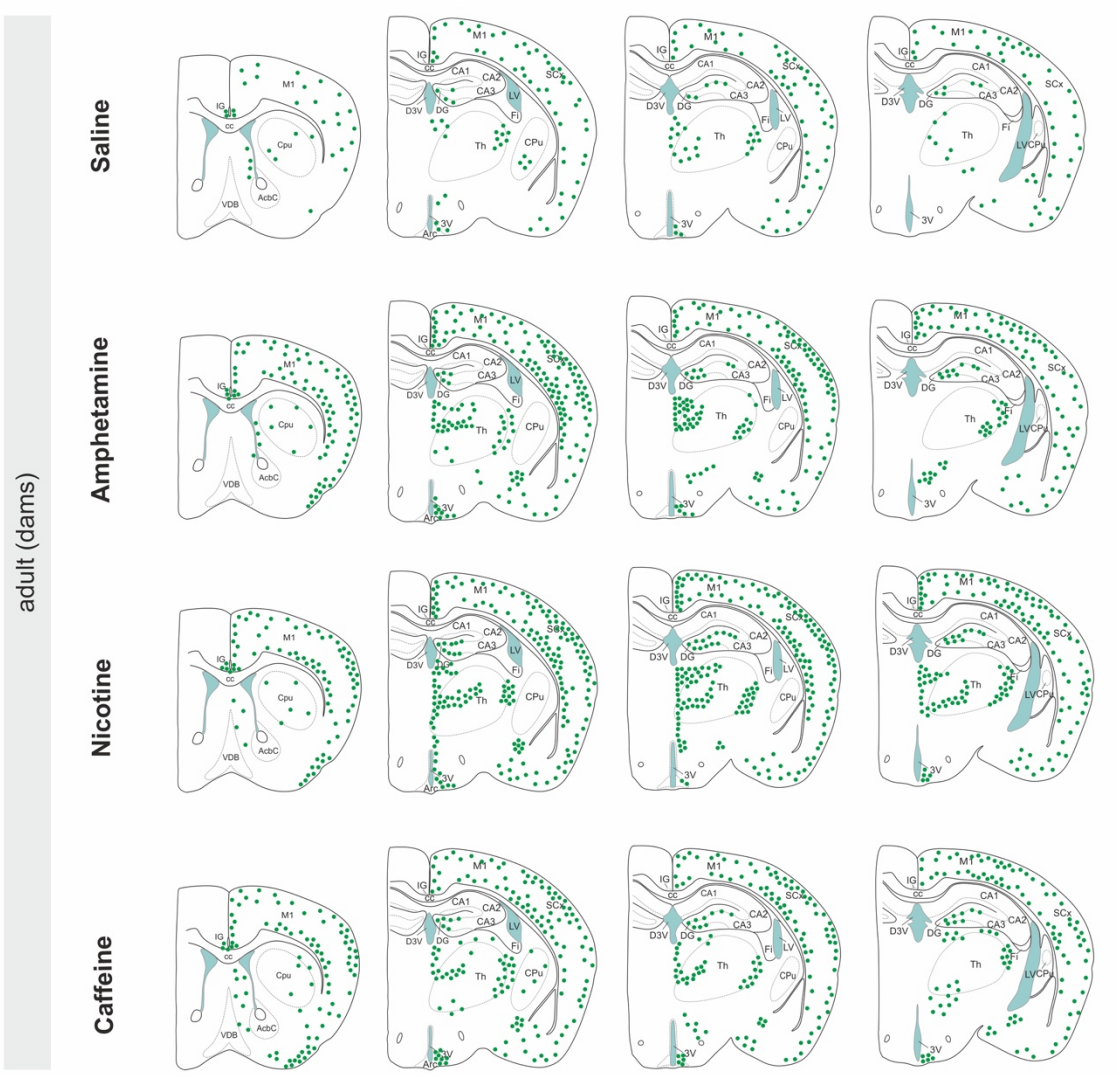

Figure S4: Cell activation maps for (adult) dams. *Fos*-CreER^{T2}::*ZsGreen1*$^{stop\text{-}floxed,stop\text{-}floxed}$ mice were treated with the psychostimulants as described (**Fig. 1A**). After 72h survival, serial brain sections were analyzed to localize *ZsGreen1*$^{+}$ somata (without histochemical signal amplification). Data are from $n \geq 3$ animals/treatment, which were mapped by at least two independent researchers blinded to the case conditions. *Abbreviations*: AcbC, core of the nucleus accumbens; ARC, arcuate nucleus; CA1-3, Cornu Ammonis 1-3 subfields of the hippocampus; cc, corpus callosum; CPu, striatum; D3V, dorsal part of the 3rd ventricle; DG, dentate gyrus; Fi, fimbria hippocampi; IG, indusium griseum; LV, lateral ventricle; M1, motor cortex; SCx, somatosensory cortex; Th, thalamus; VDB, vertical diagonal band of Broca; 3V, 3rd ventricle.

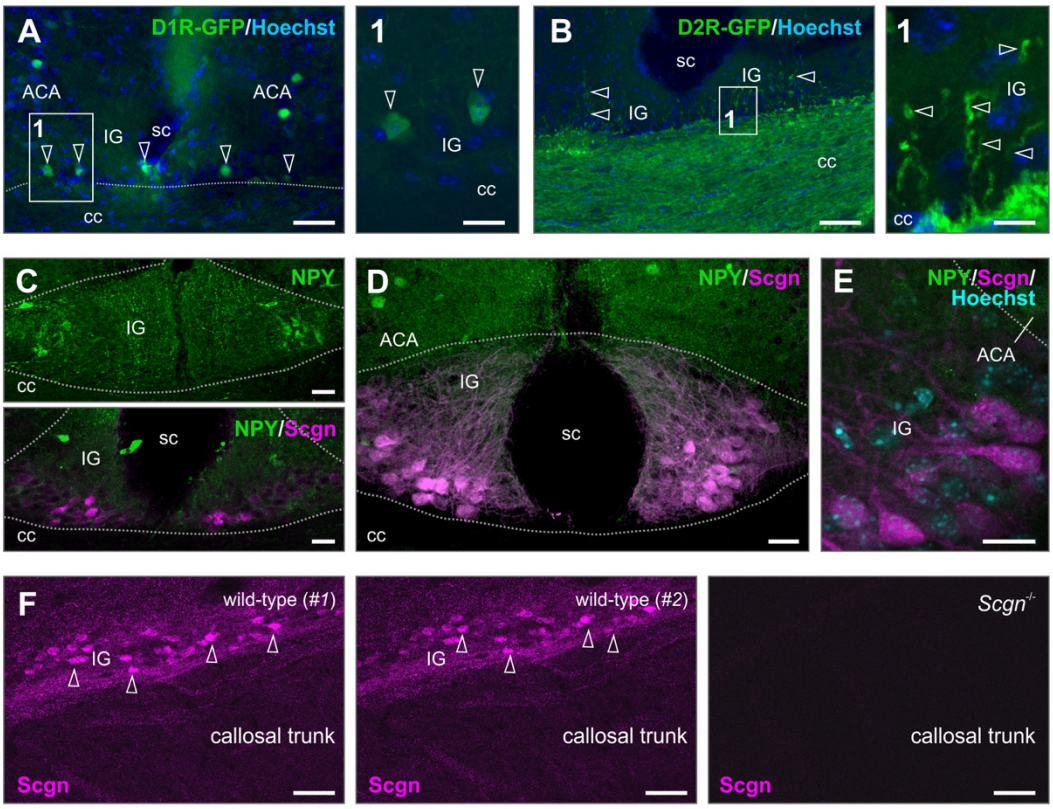

Figure S5: Neuropeptide Y (NPY) immunoreactivity during IG development. (**A,B**) Dopamine receptor 1 (D1R) and 2 (D2R) promoter controlled GFP expression in *D1R*-GFP (**A**) and *D2R*-GFP (**B**) mouse lines labels IG neurons and callosal afferents (*open arrowheads*), respectively. Enumerated rectangles denote the location of insets. Sections were counterstained with Hoechst 33,342. (**C**) NPY immunoreactivity in the putative IG on P5 shows transient neuropeptide expression in lateral cell columns (*top*). Scgn is not expressed in the IG at this time (*not shown*). By P12, the IG is NPY$^-$ with a few cells gaining Scgn immunoreactivity (*bottom*). (**D**) On P25, the IG remains essentially negative for NPY (close-up in **E**) with Scgn$^+$ neurons forming dense clusters on its ventral surface adjacent to the corpus callosum. (**F**) Scgn immunolabeling of wild-type and *Scgn*$^{-/-}$ IG supports the specificity of the novel antibody used here. *Abbreviations*: ACA, anterior cingulate area; cc, corpus callosum; IG, indusium griseum; P, postnatal day; sc sulcus centralis. *Scale bars* = 75 µm (A,B,F), 30 µm (C,D), 20 µm (A1,E), 12 µm (B1).

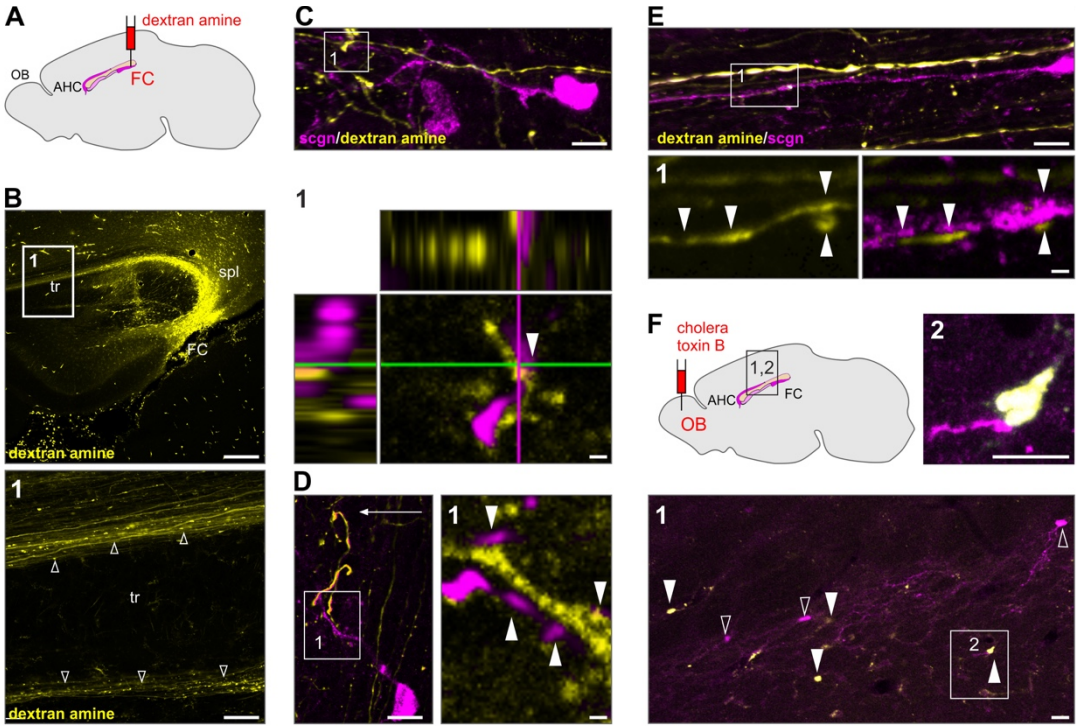

Figure S6: **Circuit organization of Scgn$^+$ IG neurons**. (**A**) Dextran amine was used as anterograde tracer and injected into the fasciola cinerea (FC) of rats. (**B**) As a result, fluorescently-labelled axons ran along the dorsal and ventral surfaces of the corpus callosum (*open arrowheads*). (**C-D**) Bouton-like fluorescently-labelled specializations were seen in close apposition to Scgn$^+$ dendrites in the IG (arrowheads in C'1', D). The lack of appreciable physical separation between pre- (dextrane amine$^+$) and postsynaptic (Scgn$^+$) neuronal compartment was verified by high-resolution orthogonal imaging (**C'1'**). (**E**) Scgn$^+$ dendrites were oriented parallel with anterogradely-traced axons and were contacted by *en passant* boutons (*arrowheads*, '1'). (**F**) Injection of cholera toxin B, a retrograde tracer, into the olfactory bulb (OB) labeled *Scgn*$^+$ neurons in the IG ('1','2'). *Abbreviations:* AHC, anterior hippocampal continuation; Scgn, secretagogin. *Scale bars* = 200 µm (B,B'1'), 50 µm (F'1'), 20 µm (E), 10 µm (C,D,F'2'), 2 µm (C'1', D'1',E'1').

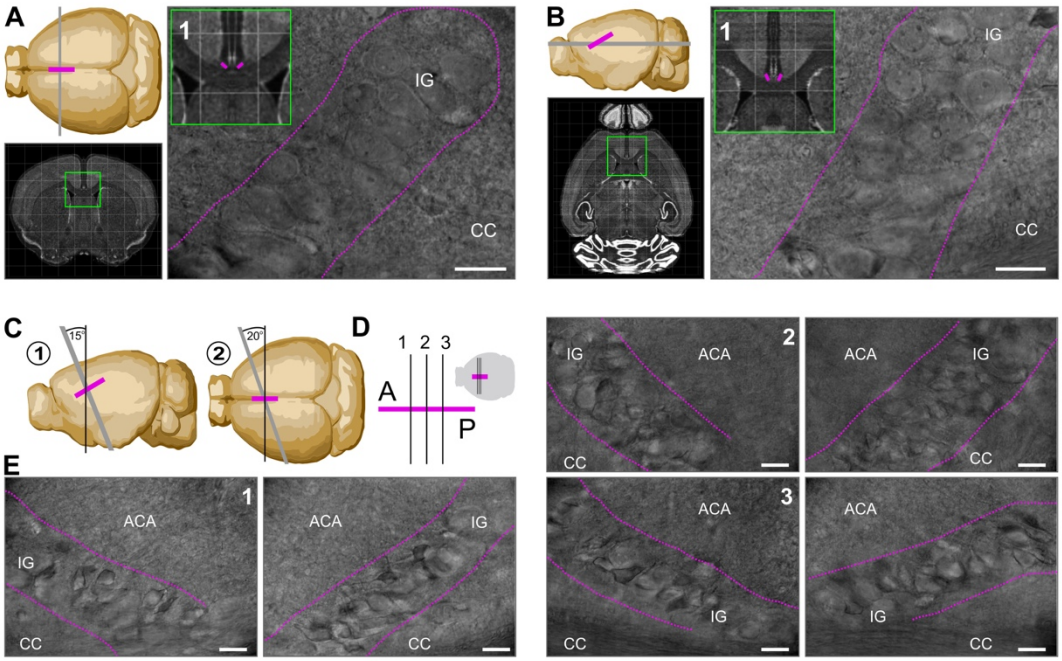

Figure S7: Cutting angle for improved neuronal survival in IG during slice preparation. (**A**) Coronal *ex vivo* brain slice preparation. Schema illustrates the coronal cutting plane (*top left*) and ensuing coronal section (*bottom left*) with the IG in magenta. (**'1'**) Differential interference microscopy (DIC) image of indusium griseum (IG) neurons in a coronal brain slice (dashed magenta line shows the boundary of this cell cluster) from the anatomical region indicated (*inset*; modified from 'Brain Explorer' of the Allen Institute). (**B**) Horizontal *ex vivo* brain slice preparation. The horizontal cutting plane (*top left*) and ensuing horizontal section (*bottom left*) are shown with magenta color indicating the location of the IG. (**'1'**) DIC image of IG neurons in a horizontal brain slice (dashed magenta line shows their physical boundary) from the anatomical region indicated (*insert*). (**C**) Para-coronal brain slice preparation. Cartoon illustrates the two steps of para-coronal brain sectioning ('1' and '2'). (**D**) Schema with the position (albeit without orientation) of para-coronal cutting planes shown in E. (**E**) DIC image of para-coronal brain slices with IG (*dashed magenta line*) in slices from the most anterior ('1') towards posterior ('3') coordinates. *Scale bars* = 10 µm.

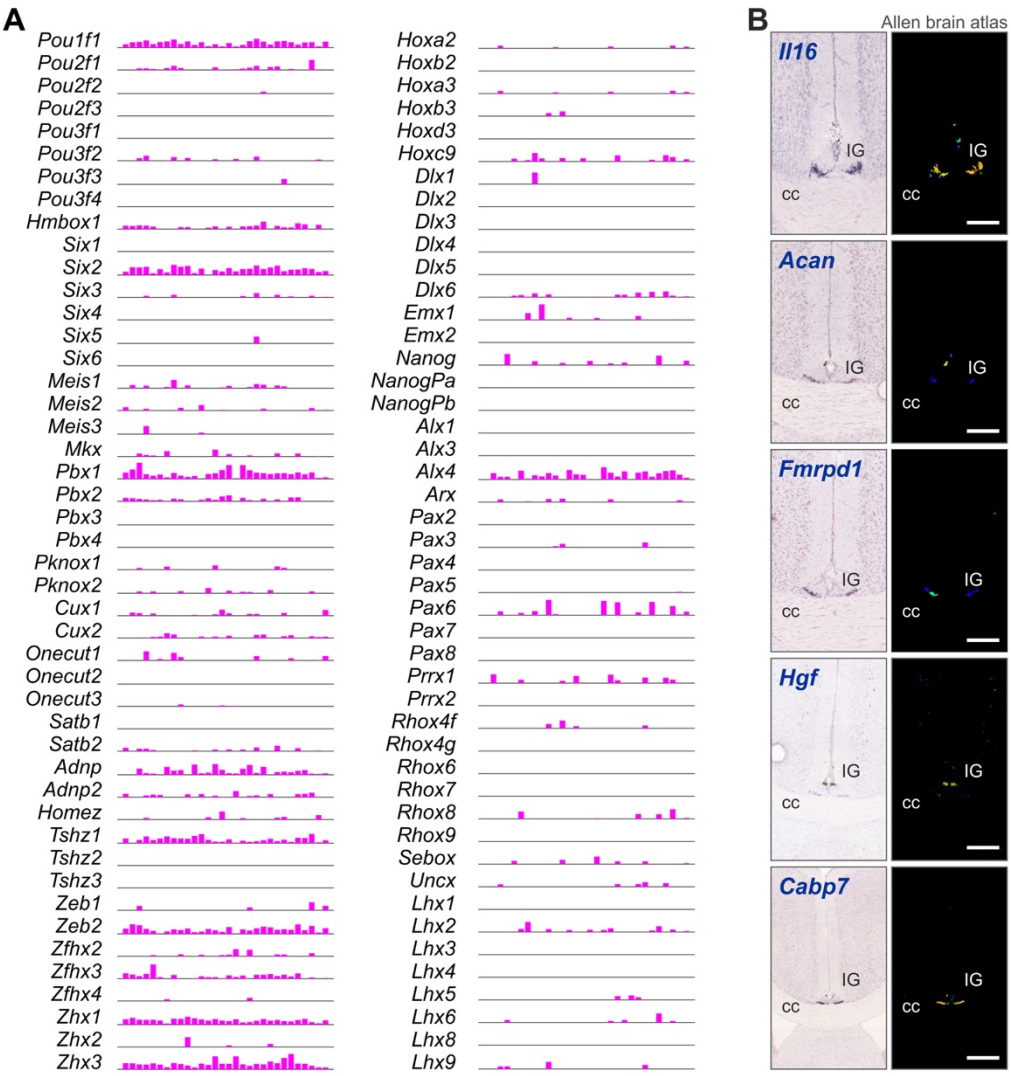

Figure S8: Transcription factor families and IG-specific markers. (**A**) Transcription factors in IG neurons probed by *Patch-seq*. Transcription factor families were plotted if at least one of the family members had been detected in >15% of the IG neurons analyzed. (**B**) IG-specific gene expression deduced from our *Patch-seq* data with the Tasic *et al*. (2016) cortical single-cell RNA-seq dataset used as reference. IG-specific enrichment was verified by surveying open-source *in situ* hybridization results from the Allen Institute (www.brain-map.org).

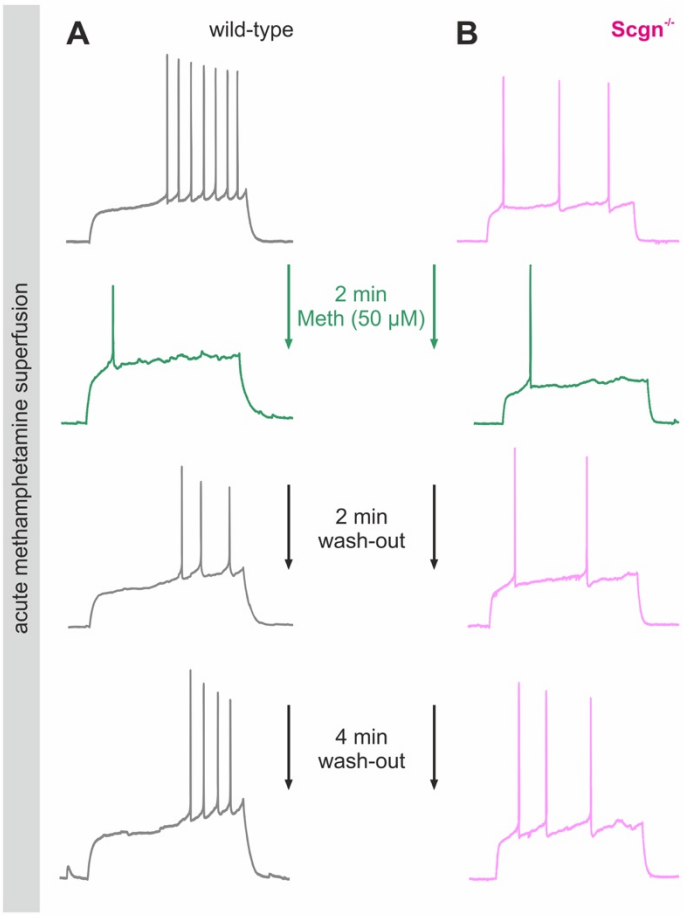

Figure S9: Acute meth-amphetamine pharmacology on wild-type and *Scgn*$^{-/-}$ IG neurons. Examples of neuronal firing upon exposure to 50 uM methamphetamine (*Meth*) superfused in the slice recording chamber. (**A)** *Meth* application on a wild-type IG neuron resulted in reduced AP formation within 2 min of superfusion. The reversible nature of *Meth* effect was verified by wash-out after 2 min. At 4 min, the firing pattern of IG neuron was comparable to that during the baseline. (**B)** *Meth* application onto *Scgn*$^{-/-}$ IG neurons resulted in an effect similar to that seen in wild-type neurons along with a comparable wash-out kinetics suggesting that *Scgn* does not impede *Meth* responsiveness acutely.

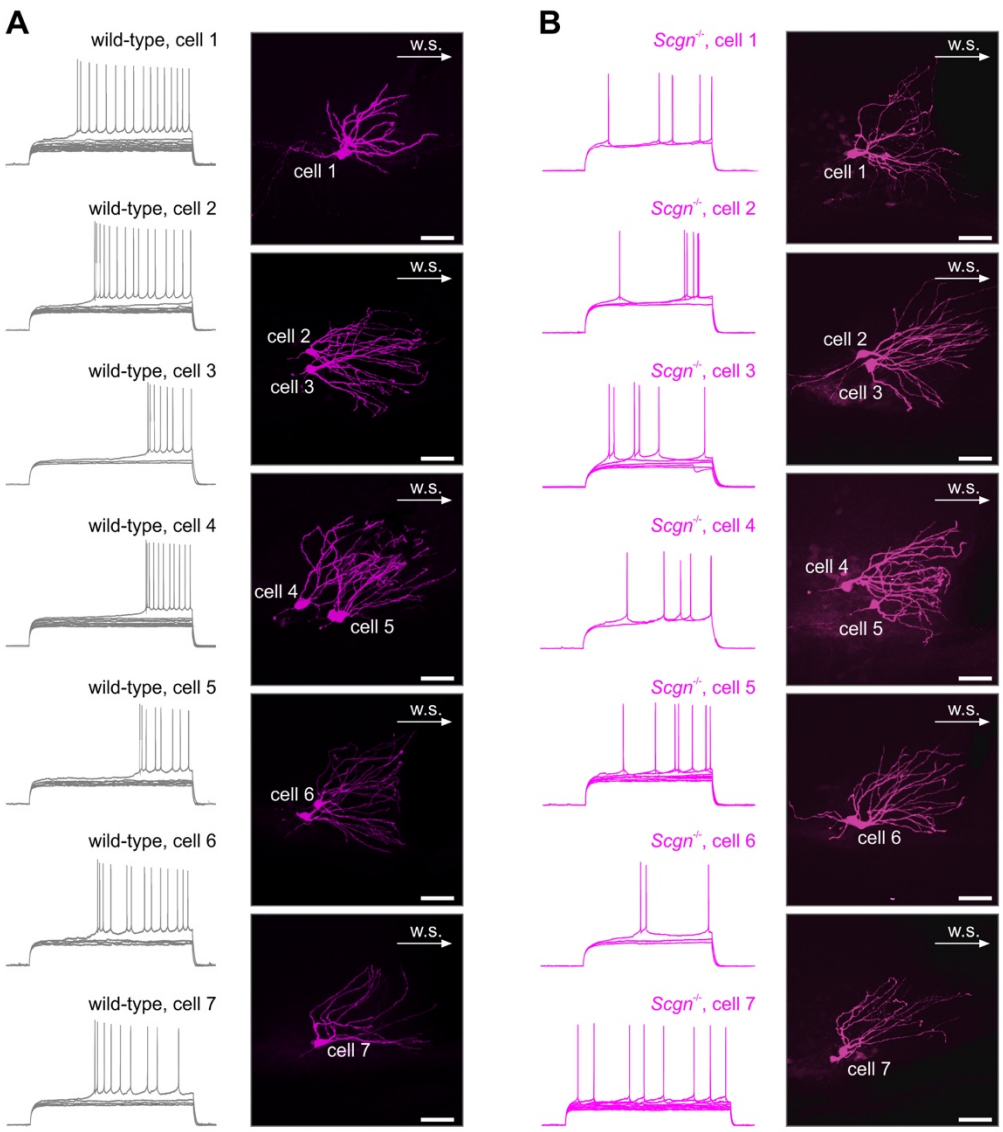

Figure S10: Examples of rheobasic firing of wild-type *vs*. *Scgn*$^{-/-}$ IG neurons. (**A**) Wild-type IG neurons displayed a delayed rheobasic activation initiated by a pre-potential (that is, a pronounced depolarization to supra-threshold membrane potential resulting in a train of APs; *left*). Corresponding neuronal morphology is shown on the right. (**B**) In contrast, a pre-potential was not appreciable in *Scgn*$^{-/-}$ IG neurons and consequently their discharge with lower rheobasic frequencies. *Scgn*$^{-/-}$ IG neuronal morphology is shown to the right; *n* = 7 neurons were selected from both groups; current steps = 2 s; *scale bars* = 20 um, arrows indicate tissue orientation and point towards the midline cortical wall surface (w.s.).

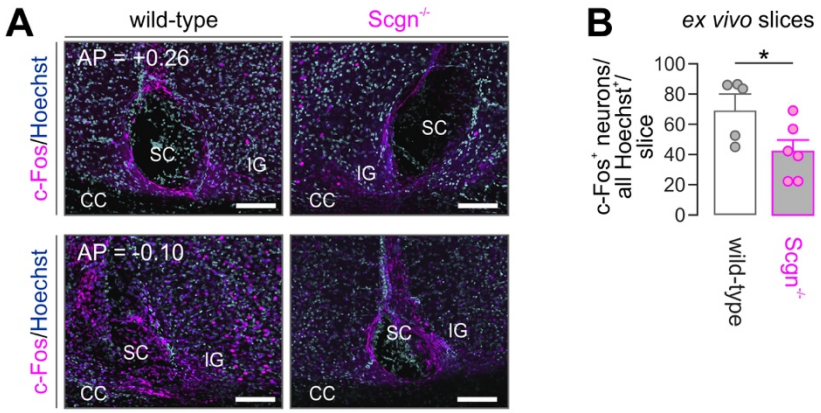

Figure S11: C-Fos activation in the postnatal IG challenged with methamphetamine. (**A**) c-Fos histochemistry in the IG of mice that had been exposed to *Meth* 24h earlier. Wild-type and *Scgn*$^{-/-}$ mice were compared. In each mouse, the quantification of c-Fos immunoreactivity (expressed as a ratio of c-Fos^{+}/all IG nuclei labeled by Hoechst staining) was performed at two anterior-posterior (AP) coordinates as shown (coordinates are relative to bregma). (**B**) Data were expressed as means ± s.e.m., n = 3 animals/group; *p < 0.05 (Student's t-test). Individual data points (2/animal at the above AP coordinates) are shown.

Captions to Supplementary Videos

Video S1: Lightsheet microscopy of a control fetal brain with residual ZsGreen1 activity.

Video S2: Lightsheet microscopy of a fetal brain with amphetamine-induced ZsGreen1 activation.

Video S3: Lightsheet microscopy of a fetal brain upon nicotine-induced ZsGreen1 activation.

Video S4: Lightsheet microscopy of a fetal brain after caffeine-induced ZsGreen1 activation.

Video S5: Methamphetamine-induced behavior of a wild-type mouse.

Video S6: Methamphetamine-induced behaviors of a *Scgn*$^{-/-}$ mouse.

Supplementary References

1. Alpar A & Harkany T (2018) Novel insights into the spatial and temporal complexity of hypothalamic organization through precision methods allowing nanoscale resolution. *J Internal Med* 284:568-580.
2. Calvigioni D*, et al.* (2017) Functional Differentiation of Cholecystokinin-Containing Interneurons Destined for the Cerebral Cortex. *Cereb Cortex* 27:2453-2468.
3. Guenthner CJ, Miyamichi K, Yang HH, Heller HC, & Luo L (2013) Permanent genetic access to transiently active neurons via TRAP: targeted recombination in active populations. *Neuron* 78:773-784.
4. Fuzik J*, et al.* (2016) Integration of electrophysiological recordings with single-cell RNA-seq data identifies neuronal subtypes. *Nat Biotechnol* 34:175-183.
5. Susaki EA*, et al.* (2014) Whole-brain imaging with single-cell resolution using chemical cocktails and computational analysis. *Cell* 157:726-739.
6. Romanov RA*, et al.* (2017) Molecular interrogation of hypothalamic organization reveals distinct dopamine neuronal subtypes. *Nat Neurosci* 20:176-188.
7. Schnell SA, Staines WA, & Wessendorf MW (1999) Reduction of lipofuscin-like autofluorescence in fluorescently labeled tissue. *J Histochem Cytochem* 47:719-730.
8. Rogers DC*, et al.* (1997) Behavioral and functional analysis of mouse phenotype: SHIRPA, a proposed protocol for comprehensive phenotype assessment. *Mamm Genome* 8:711-713.
9. Rogers DC*, et al.* (2001) SHIRPA, a protocol for behavioral assessment: validation for longitudinal study of neurological dysfunction in mice. *Neurosci Lett* 306:89-92.
10. Tasic B, Menon V, & Nguyen TN (2016) Adult mouse cortical cell taxonomy revealed by single cell transcriptomics. *Nat Neurosci* 19:335-346.